How to cite: *Angew. Chem. Int. Ed.* **2023**, *62*, e202309566
doi.org/10.1002/anie.202309566

VIP **Radical Stability** *Very Important Paper*

MIDA- and TIDA-Boronates Stabilize α-Radicals Through B–N Hyperconjugation

Antonio J. LaPorte, Jack E. Feldner, Jan C. Spies, Tom J. Maher, and Martin D. Burke**

Abstract: Multifunctional organoboron compounds increasingly enable the simple generation of complex, Csp^3-rich small molecules. The ability of boron-containing functional groups to modify the reactivity of α-radicals has also enabled a myriad of chemical reactions. Boronic esters with vacant p-orbitals have a significant stabilizing effect on α-radicals due to delocalization of spin density into the empty orbital. The effect of coordinatively saturated derivatives, such as N-methyliminodiacetic acid (MIDA) boronates and counterparts, remains less clear. Herein, we demonstrate that coordinatively saturated MIDA and TIDA boronates stabilize secondary alkyl α-radicals via $\sigma_{B\text{-}N}$ hyperconjugation in a manner that allows site-selective C–H bromination. DFT calculated radical stabilization energies and spin density maps as well as LED NMR kinetic analysis of photochemical bromination rates of different boronic esters further these findings. This work clarifies that the α-radical stabilizing effect of boronic esters does not only proceed via delocalization of radical character into vacant boron p-orbitals, but that hyperconjugation of tetrahedral boron-containing functional groups and their ligand electron delocalizing ability also play a critical role. These findings establish boron ligands as a useful dial for tuning reactivity at the α-carbon.

Multifunctional organoboron compounds have transformed strategies for the synthesis of complex small molecules, including in an automated manner.[1–25] The ability of boryl groups to modify the reactivity of α-radicals has played a critical role in the development of new reactions.[26–28] Powerful chemical transformations involving α-boryl radicals are reported frequently, including radical addition to vinyl boronates (Scheme 1A),[29–31] addition of α-boryl radicals to alkenes (Scheme 1B),[32–34] cross-coupling reactions (Scheme 1C), and more.[26,35–40] Notably, the nature of the boryl group is crucial for achieving desired reactivity,[41–43] an effect that has been attributed to differential radical stabilizing abilities between boryl functional groups.[44] Specifically, it has been proposed that boryl groups with a vacant p-orbital, such as pinacol boronic esters, stabilize α-radicals via a π-bonding, spin delocalization interaction.[45–46] Meanwhile, the effect boronic esters with filled p-orbitals, such as N-methyliminodiacetic acid (MIDA) boronates and derivatives, remains less clear. In fact, some have even proposed that these boronates have no stabilizing effect.[42] However, recent evidence has emerged that suggests MIDA boronate groups could affect notable stabilization of α-radicals. Wang and co-workers demonstrated in a competition experiment that bromination of a benzylic MIDA boronate is favored over a tolyl methyl group, and that cyclohexyl MIDA boronate can be site-selectively brominated at the α-boryl position, although in only 13 % yield.[48] The mechanisms and relative magnitudes by which boryl groups stabilize α-radicals are not fully understood. Advancing such understandings and systematic benchmarking of relative radical stabilizing abilities of diverse, synthetically useful boron-containing functional groups would be highly enabling for the development of new reactions that proceed via α-boryl radical intermediates.

Here we computationally demonstrate that coordinatively saturated boronates stabilize α-radicals (Scheme 1D), corroborate this by developing a site-selective C–H bromination reaction, and show by LED NMR kinetic analysis that photochemical bromination rates of different alkyl boronic esters correlate with their radical stabilization energies. These findings identify boron ligand structure as a powerful dial for tuning radical reactivity at the α-carbon.

To clarify the relative radical stabilizing abilities of MIDA boronates, their recently reported tetramethylated variant (TIDA boronates), and other synthetically relevant boryl groups, we used DFT to calculate their radical

[*] A. J. LaPorte, J. E. Feldner, J. C. Spies, T. J. Maher, Prof. M. D. Burke
Department of Chemistry, University of Illinois
Urbana, IL 61820 (USA)
E-mail: laporte3@illinois.edu
mdburke@illinois.edu
Prof. M. D. Burke
Carle Illinois College of Medicine, University of Illinois
Urbana, IL 61820 (USA)
and
Department of Biochemistry, University of Illinois
Urbana, IL 61820 (USA)
and
Arnold and Mable Beckman Institute, University of Illinois
Urbana, IL 61820 (USA)
and
Carl R. Woese Institute for Genomic Biology, University of Illinois
Urbana, IL 61820 (USA)

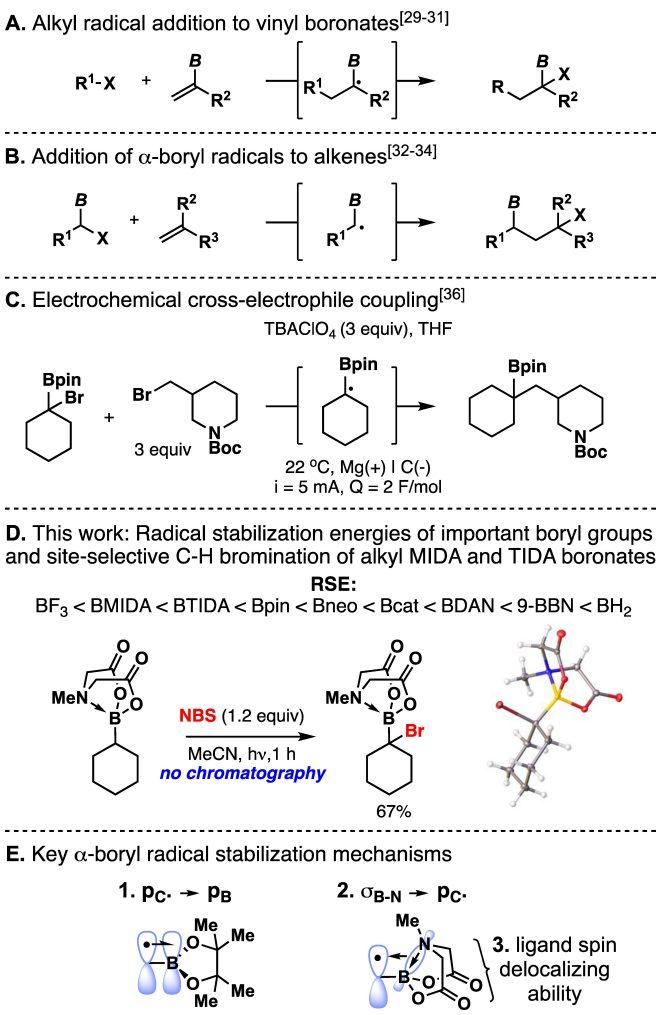

Scheme 1. α-Boryl radicals are important reaction intermediates, and their stability/reactivity is highly dependent on boryl group structure. ***B*** indicates boryl group.

stabilization energies (RSE).[44,46,47,49–52] RSE is determined by subtracting the bond dissociation energy (BDE) of methane from that of the corresponding substituted methane. Density functional theory at the M06-2X/def2-TZVP level was used to calculate C–H BDEs of methanes with a series of substituents including Me, BF_3, BMIDA, BTIDA, Bpin, Bcat, BDAN, 9-BBN, BH_2, and Ph (Figure 1A).[53] Simultaneously, spin density maps were computed to visualize the delocalization of unpaired electron density throughout boryl groups, and NBO spin population analysis was performed to quantify unpaired electron density. M06-2X/def2-TZVP level of theory was chosen as it has been shown to be both accurate and not computationally prohibitive for determination of BDEs.[52,54] We found that the trifluoroborate substituent provided less stabilization than a methyl group (3.2 vs 4.0 kcal/mol).[55] The lack of a vacant boron p-orbital, but presence of spin density on fluorine atoms and syn-periplanar alignment of $\sigma_{B\text{-}F}$ and p_C, suggests that some stabilizing effect arises via hyperconjugation.

The MIDA boronate substituent exhibited a RSE of 4.6 kcal/mol, supporting that MIDA boronates have a substantial stabilizing effect on α-radicals, even with the lack of a vacant boron p-orbital. This stabilization likely arises from hyperconjugation of the MIDA boronate B–N bond into p_C ($\sigma_{B\text{-}N} \rightarrow p_C$).[56,57] This is supported by the lengthening of the calculated B–N bond from 1.69 Å to 1.72 Å for the parent compound and radical respectively. Spin delocalization throughout the MIDA backbone suggests that the structure of the ligand could have a substantial impact on radical stability, regardless of boron p-orbital availability. Furthering this, the TIDA boronate substituent imparted 6.1 kcal/mol of stabilization energy, 1.5 kcal/mol more than the MIDA boronate, also arising from B–N hyperconjugation ($\sigma_{B\text{-}N} \rightarrow p_C$). Quantum theory of atoms in molecules (QTAIM)-based charge density analysis of MIDA and TIDA boronate X-ray crystal structures previously revealed increased hyperconjugation within the TIDA boronate cage that yielded enhanced chemical stability relative to MIDA boronates under a variety of reaction conditions.[58] This increased ability to delocalize electron density can be observed in the BTIDA α-boryl radical spin density map, where 40 % more unpaired electron density is observed on the TIDA backbone relative to the MIDA backbone, and this increased spin density is localized on one of the TIDA methyl groups that, due to torsion of the TIDA cage, is positioned above the carbon radical center (Figure 1B). Additionally, the calculated TIDA boronate B–N bond length increased from 1.68 Å to 1.69 Å for the parent compound and radical respectively. This further supports that the structure of the boryl group's ligand has a substantial impact on α-radical stabilizing ability, regardless of boron p-orbital availability. Furthermore, both MIDA and TIDA boronates show asymmetric distribution of spin throughout the boryl ligands due to torsion of their respective cages that we speculate is a consequence of steric strain.

Pinacol and neopentyl glycol boronic ester groups showed RSE values of 6.7 and 7.0 kcal/mol respectively, consistent with increased boron p-orbital availability allowing for a favorable π-bonding interaction. Radical stabilization is further enhanced by incorporating aromatic rings into the ester backbone, as seen with Bcat and BDAN substituents that exhibited 7.4 and 7.5 kcal/mol RSE respectively. Spin density maps revealed that delocalization of radical character into the aromatic rings is likely responsible for increased RSE. Finally, 9-BBN and BH_2 exhibited RSE of 10.2 and 11.6 respectively, the highest of the organoboron groups tested, as expected due to greatest p-orbital availability.

Next, we asked how location of spin density affects RSE by performing NBO spin population analysis on the set of boromethyl radicals. Increased spin population on the carbon baring radical indicates lower RSE, as expected, due to greater localization of charge (Figure 1C). Individually, spin density present on the boron atom or on the ligand are not useful predictors of RSE (Figure 1C and D), but summation of spin density absolute value across boron and ligand atoms yields a notable correlation with RSE (Fig-

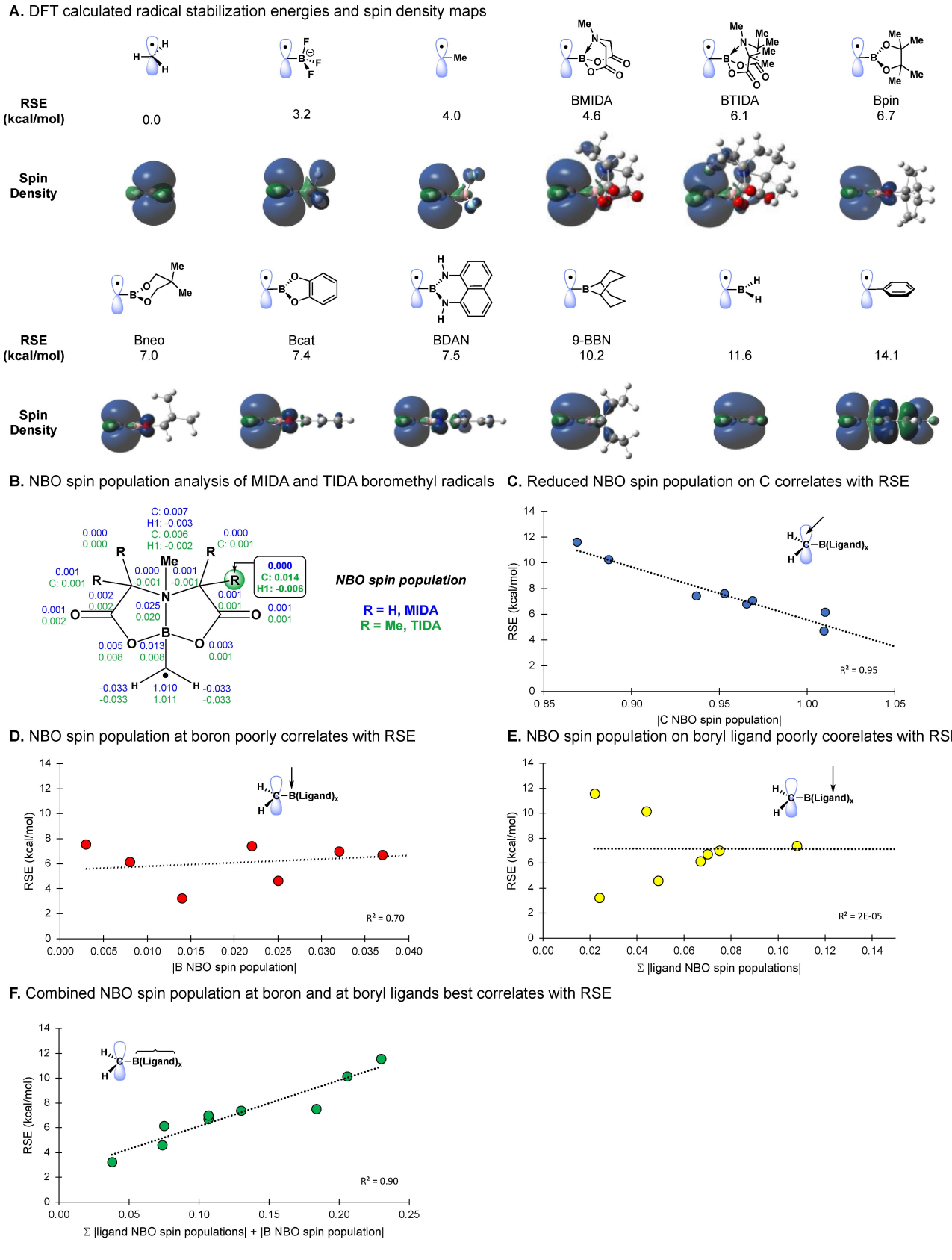

Figure 1. Radical stabilization energies, spin density maps, and relationship between NBO spin location and RSE for synthetically important boryl groups. Spin density maps generated with isovalue: MO = 0.02, density = 0.0006. Geometry optimization: B3LYP-D3BJ/6-31 + + G(d,p), gas phase. RSE calculations, spin density maps, NBO spin population analysis: M06-2X/def2-TZVP, gas phase. Hydrogens with NBO spin population less than 0.000 were excluded from **D**. Σ|ligand NBO spin populations| represents the summation of absolute values of the NBO spin population of each atom.

Table 1: Site-selective photochemical C–H bromination of alkyl MIDA and TIDA boronates.

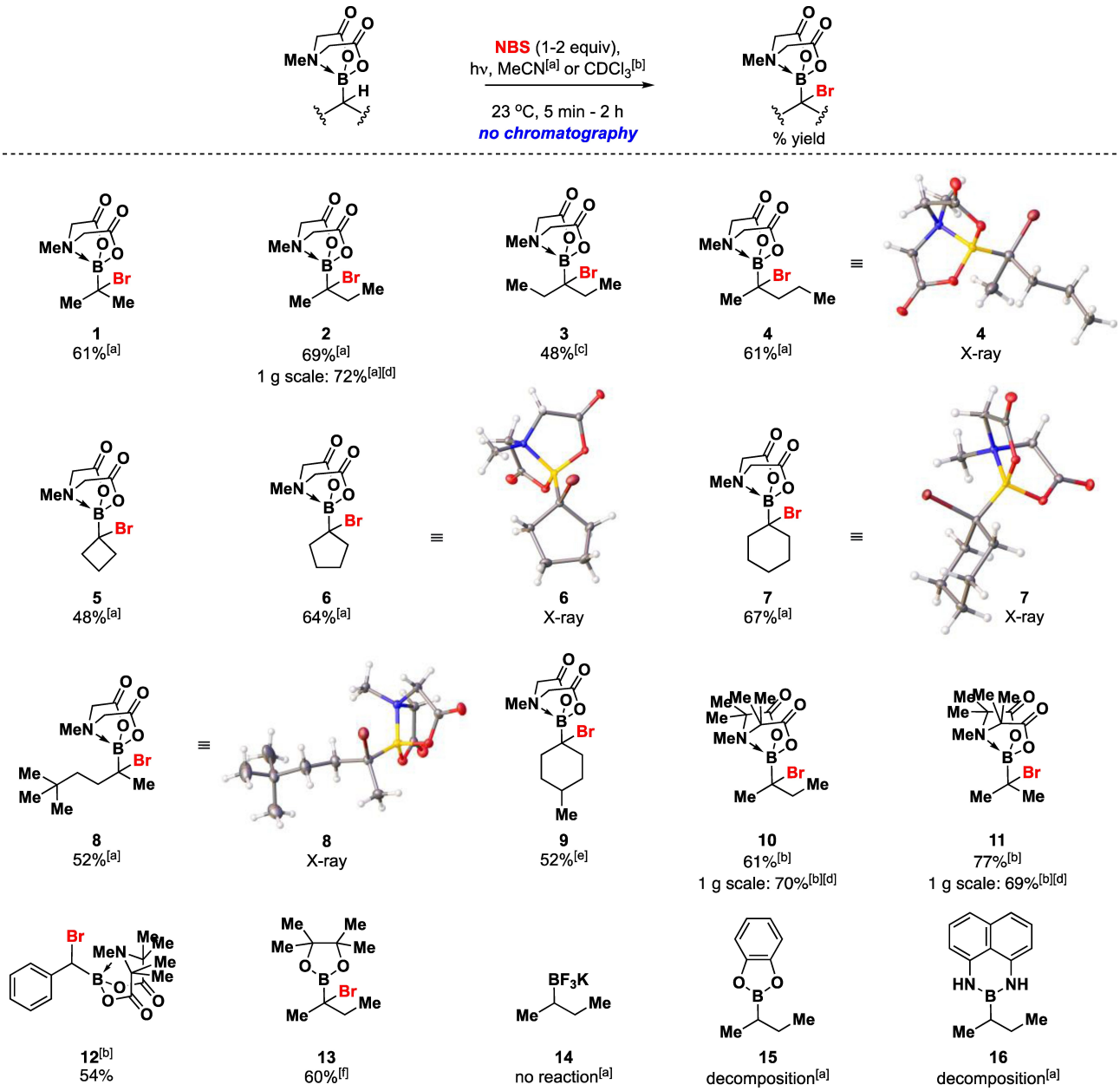

[a] General procedure for bromination of MIDA boronates: Reactions were performed on a 0.5 mmol scale in MeCN at a concentration of 0.125 M. Brominated products were isolated by crystallization from crude reaction mixtures. [b] General procedure for bromination of TIDA boronates: Reactions were performed on a 0.5 mmol scale in chloroform-d at a concentration of 0.125 M. Brominated products were isolated by crystallization from crude reaction mixtures. [c] The general procedure for bromination of MIDA boronates was followed but on a 0.25 mmol scale. [d] The reaction was performed with 1.0 g of MIDA or TIDA boronate and scaled accordingly based on respective general procedures. [e] The general procedure for bromination of MIDA boronates was followed except with dichloromethane as the solvent. Relative stereochemistry was not determined. [f] The general procedure for bromination of MIDA boronates was followed but the product was purified by concentration of the crude reaction mixture, dissolving in pentane, and filtering through celite.

ure 1F). This suggests that boryl ligand spin delocalizing ability plays a critical role in the RSE of boryl groups beyond simply modulating the availability of the boron p-orbital.

Having shown computationally that MIDA and TIDA boronates impart significant stabilization on α-radicals, we asked if this effect could be leveraged in a synthetically useful manner by developing a reaction that requires radical stabilization for high degrees of efficiency and site selectivity.[59–66] The site-selective C–H bromination of secondary alkyl MIDA boronates served as an excellent model system, as there are no synthetically efficient examples of this reaction. After brief reaction optimization (SI page 6), we found that a variety of secondary alkyl MIDA boronates

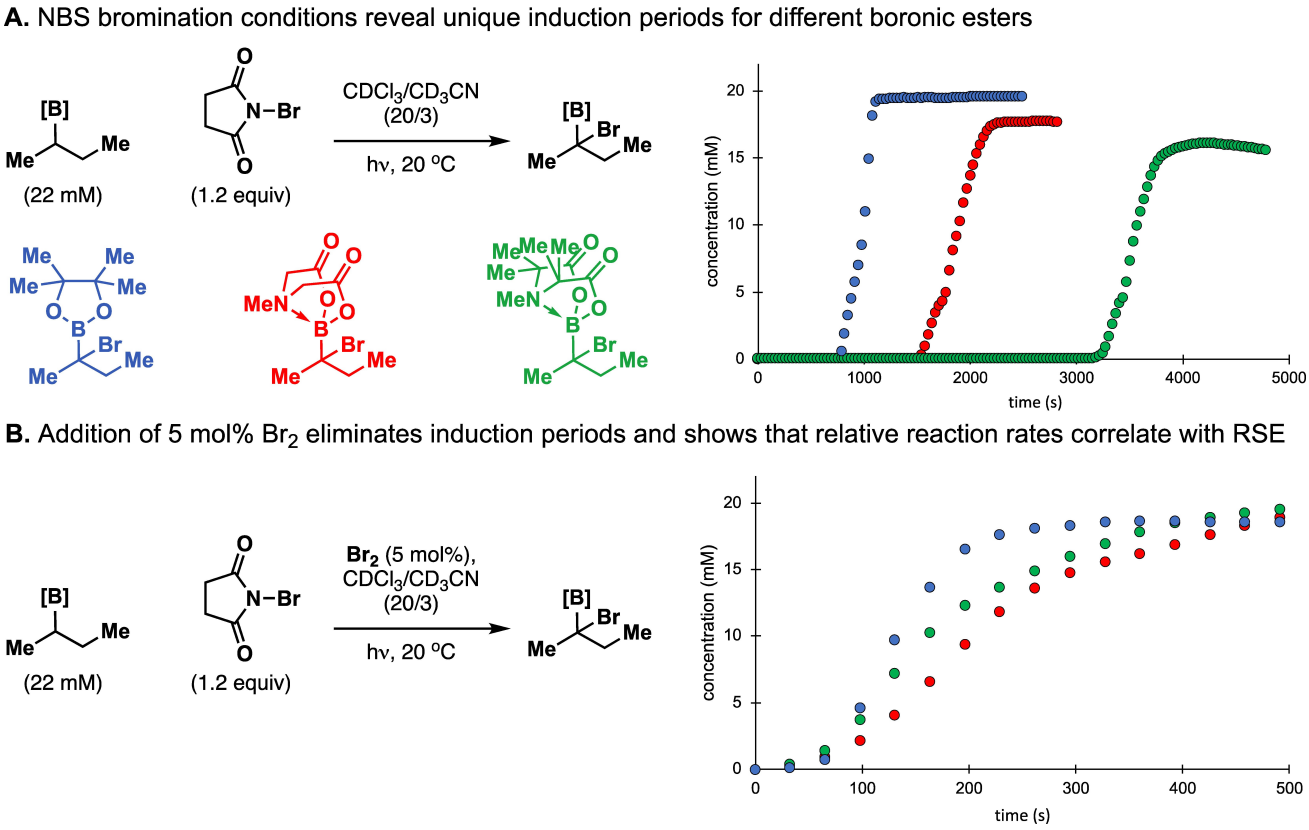

Figure 2. LED NMR kinetic analysis of site-selective photochemical C–H bromination reaction. A $CDCl_3/CD_3CN$ solvent mixture was required to allow reaction of all boronic esters under the same reaction conditions.

undergo site-selective photochemical bromination at the α-boryl position using 1–2 equivalents of NBS in acetonitrile while irradiating with white light for 1–2 hours, and brominated products could be purified via direct crystallization from crude reaction mixtures (Table 1). These compounds are crystalline, bench stable solids.[67] Other secondary positions are not affected by the bromination reaction, and compound **9**, containing a tertiary C–H bond, still underwent selective bromination at the α-boryl position. *n*-Butyl MIDA boronate was submitted to bromination conditions and no reaction occurred, suggesting that primary alkyl MIDA boronates are not reactive under these conditions. We also tested the bromination of alkyl MIDA boronate substrates containing oxygen and nitrogen substituents capable of stabilizing α-radicals but only observed unidentifiable byproducts and none of the desired bromination products.

Recently, our group showed that TIDA boronates exhibit remarkable chemical stability relative to MIDA boronates under a variety of reaction conditions.[58] Our calculations suggest that TIDA boronates provide an additional 1.5 kcal/mol of stabilization relative to MIDA boronates, indicating that secondary alkyl TIDA boronates should also be competent substrates for the bromination reaction. Submission of *sec*-butyl BTIDA under our general conditions yielded decomposition. However, changing solvents from acetonitrile to $CDCl_3$ allowed for the successful bromination of secondary alkyl TIDA boronates in as fast as 5 minutes. Deuterated chloroform was used to check for reaction completion by ^{1}H NMR as some reactions completed in under five minutes. α-Bromo TIDA boronates are also crystalline solids that can be purified via crystallization from the crude reaction mixture. Additionally, both alkyl MIDA and TIDA boronates were brominated on gram scales. *Sec*-butyl Bpin underwent clean bromination under the NBS bromination conditions. S*ec*-butyl BF_3K was unreactive under the conditions and attempts to brominate *sec*-butyl BDAN and *sec*-butyl Bcat yielded only unidentifiable decomposition products that we speculate arise from aromatic bromination.

Having shown that MIDA and TIDA boronates provide a radical stabilizing effect significant enough to enable otherwise inaccessible reactivity, we asked if calculated radical stabilization energies could be used to predict the relative photochemical bromination reaction rates of *sec*-butyl MIDA, TIDA, and pinacol boronic esters. The Hammond postulate suggests that for an endergonic reaction with a late transition state, such as the rate-limiting C–H abstraction step in free radical bromination, the transition state more closely resembles the product than the starting material.[68–71] Thus, we expected a lower energy α-boryl radical formed after C–H abstraction should affect a lower energy transition state and therefore faster reaction rate. Lack of useful chromophores made secondary alkyl

boronic esters challenging to visualize by HPLC, so we turned to nuclear magnetic resonance spectroscopy with an intra-sample light emitting diode as the white light source (LED NMR).[72–76] We constructed a custom LED NMR setup that we maintain is the cheapest, simplest, and most accessible device reported to date that can be quickly assembled and employed in any laboratory with an NMR spectrometer. A parts list and assembly instructions with pictures are provided in the Supporting Information (pages 22–32). An additional challenge we faced was that alkyl TIDA boronates required chloroform as the bromination solvent, but MIDA boronates were insoluble. To overcome this, we found that a 20/3 mixture of $CDCl_3/CD_3CN$ was a productive bromination solvent for pinacol, MIDA, and TIDA boronic esters.

With bromination conditions and an LED NMR apparatus in hand, we began our kinetics experiments (Figure 2). In our first experiments we observed variable induction periods for the different boronic esters, indicating different initiation times, but relative propagation rates followed the order Bpin > BTIDA > BMIDA (Figure 2A). This was not surprising, as induction periods are common for Wohl-Ziegler-type bromination reactions, and it is well documented that differences in initiation time can occur due to subtle variation in radical scavenging species, acid, and other factors.[77–80] To compare relative rates more directly, we aimed to eliminate variability in initiation times. Quasdorf and co-workers showed recently that addition of substoichiometric quantities of Br_2 to a benzylic bromination reaction mediated by NBS eliminated observed induction periods.[80] By adding 5 mol % Br_2 to our LED NMR experiments we observed disappearance of induction period for all boronic esters tested, and observed relative rates of Bpin > BTIDA > BMIDA supporting that RSEs can be used to make meaningful predictions of reactivity (Figure 2B).

In summary, we have demonstrated the first conclusive evidence that coordinatively saturated MIDA and TIDA boronates stabilize α-radicals by calculating radical stabilization energies and spin density maps using density functional theory, by leveraging this new-found knowledge to develop a site-selective C–H bromination reaction, and developing a simple LED NMR apparatus that allowed us to demonstrate that relative bromination rates of different boronic esters correlate with calculated RSEs. This work clarifies that the α-radical stabilizing effect of boryl groups does not only proceed via delocalization of radical character into vacant boron p-orbitals, but that hyperconjugation of tetrahedral boryl groups, and their electron delocalizing ability, also play important roles, identifying boryl ligands as a functional dial for tuning desired radical reactivity at the α-carbon. Additionally, the α-bromoboronates generated using the reported bromination reaction likely have diverse potential for further derivatization and reaction development that our laboratory is currently pursuing.

Supporting Information

The authors have cited additional references within the Supporting Information.[81–85]

Acknowledgements

A.J.L. acknowledges Professor Jeffrey Bjorklund, Professor David Rausch, Professor Jason Hein, Dr. Dean Olson, Dr. Leonidas-Dimitrios Syntrivanis and Dr. Theodore Tyrikos-Ergas for helpful discussions. Wesley Wang is acknowledged for NMR kinetics training. A.J.L., J.E.F., J.C.S., T.J.M., and M.D.B. acknowledge the UIUC SCS mass spectrometry, NMR, and X-ray facilities for their assistance. The Roy J. Carver Charitable Trust of Muscatine, Iowa, is acknowledged for financially supporting the purchase of the B500 Bruker Avance III HD NMR spectrometer used throughout this work. The NSF is gratefully acknowledged for financial support (NSF CHE 1955838).

Conflict of Interest

The University of Illinois has filed patent applications related to MIDA and TIDA boronates with M.D.B. as an inventor.

Data Availability Statement

The data that support the findings of this study are available in the supplementary material of this article.

Keywords: Boronates · Bromination Reaction · DFT Calculations · NMR Apparatus · Radical Stability

[1] J. W. Lehmann, D. J. Blair, M. D. Burke, *Nat. Chem. Rev.* **2018**, *2*, 0115.
[2] M. Trobe, M. D. Burke, *Angew. Chem. Int. Ed.* **2018**, *57*, 4192–4214.
[3] J. W. B. Fyfe, A. J. B. Watson, *Chem* **2017**, *3*, 31–55.
[4] A. J. J. Lennox, G. C. Lloyd-Jones, *Chem. Soc. Rev.* **2014**, *43*, 412–443.
[5] Z. He, A. K. Yudin, *J. Am. Chem. Soc.* **2011**, *133*, 13770–13773.
[6] Z. He, P. Trinchera, S. Adachi, J. D. St. Denis, A. K. Yudin, *Angew. Chem. Int. Ed.* **2012**, *51*, 11092–11096.
[7] W. Shao, S. J. Kaldas, A. K. Yudin, *Chem. Sci.* **2017**, *8*, 4431–4436.
[8] C. F. Lee, D. B. Diaz, A. Holownia, S. J. Kaldas, S. K. Liew, G. E. Garrett, T. Dudding, A. K. Yudin, *Nat. Chem.* **2018**, *10*, 1062–1070.
[9] A. Holownia, C. Tien, D. B. Diaz, R. T. Larson, A. K. Yudin, *Angew. Chem. Int. Ed.* **2019**, *58*, 15148–15153.
[10] C. H. Tien, A. Trofimova, A. Holownia, B. S. Kwak, R. T. Larson, A. K. Yudin, *Angew. Chem. Int. Ed.* **2021**, *60*, 4342–4349.
[11] W. Ming, H. S. Soor, X. Liu, A. Trofimova, A. K. Yudin, T. B. Marder, *Chem. Soc. Rev.* **2021**, *50*, 12151–12188.

[12] V. Trudel, C. Brien, J. Tan, A. K. Yudin, *Chem. Commun.* **2022**, *58*, 5033–5036.
[13] J. Lozada, Z. Liu, D. M. Perrin, *J. Org. Chem.* **2014**, *79*, 5365–5368.
[14] M. L. Lepage, S. Lai, N. Peressin, R. Hadjerci, B. O. Patrick, D. M. Perrin, *Angew. Chem. Int. Ed.* **2017**, *56*, 15257–15261.
[15] J. Lozada, W. Xuan Lin, R. M. Cao-Shen, R. Astoria Tai, D. M. Perrin, *Angew. Chem. Int. Ed.* **2023**, *62*, e202215371.
[16] J. W. B. Fyfe, E. Valverde, C. P. Seath, A. R. Kennedy, J. M. Redmond, N. A. Anderson, A. J. B. Watson, *Chem. Eur. J.* **2015**, *21*, 8951–8964.
[17] C. W. Muir, J. C. Vantourout, A. Isidro-Llobet, S. J. F. Macdonald, A. J. B. Watson, *Org. Lett.* **2015**, *17*, 6030–6033.
[18] J. J. Molloy, C. P. Seath, M. J. West, C. McLaughlin, N. J. Fazakerley, A. R. Kennedy, D. J. Nelson, A. J. B. Watson, *J. Am. Chem. Soc.* **2018**, *140*, 126–130.
[19] G. E. Bell, J. W. B. Fyfe, E. M. Israel, A. M. Z. Slawin, A. Cam, A. J. B. Watson, *Org. Lett.* **2022**, *24*, 3024–3027.
[20] K. A. C. Bastick, A. J. B. Watson, *ACS Catal.* **2023**, *13*, 7013–7018.
[21] J. M. Halford-McGuff, D. B. Cordes, A. J. B. Watson, *Chem. Commun.* **2023**, *59*, 7759–7762.
[22] D. Leonori, V. K. Aggarwal, *Acc. Chem. Res.* **2014**, *47*, 3174–3183.
[23] C. Sandford, V. K. Aggarwal, *Chem. Commun.* **2017**, *53*, 5481–5494.
[24] R. J. Armstrong, V. K. Aggarwal, *Synthesis* **2017**, *49*, 3323–3336.
[25] B. S. L. Collins, C. M. Wilson, E. L. Myers, V. K. Aggarwal, *Angew. Chem. Int. Ed.* **2017**, *56*, 11700–11733.
[26] T. Taniguchi, *Chem. Eur. J.* **2022**, *28*, e202104333.
[27] A. Marotta, C. E. Adams, J. J. Molloy, *Angew. Chem. Int. Ed.* **2022**, *61*, e202207067.
[28] M. Kischkewitz, F. W. Friese, A. Studer, *Adv. Synth. Catal.* **2020**, *362*, 2077–2087.
[29] H. Lopez-Ruiz, S. Z. Zard, *Chem. Commun.* **2001**, 2618–2619.
[30] M. R. Heinrich, L. A. Sharp, S. Z. Zard, *Chem. Commun.* **2005**, 3077–3079.
[31] M. Kischkewitz, C. Gerleve, A. Studer, *Org. Lett.* **2018**, *20*, 3666–3669.
[32] R. A. Batey, B. Pedram, K. Yong, G. Baquer, *Tetrahedron Lett.* **1996**, *37*, 6847–6850.
[33] R. A. Batey, D. V. Smil, *Tetrahedron Lett.* **1999**, *40*, 9183–9187.
[34] A. Marotta, H. Fang, C. E. Adams, K. S. Marcus, C. G. Daniliuc, J. Molloy, *Angew. Chem. Int. Ed.* **2023**, *62*, e202307540.
[35] J. Schmidt, J. Choi, A. T. Liu, M. Slusarczyk, G. C. Fu, *Science* **2016**, *354*, 1265–1269.
[36] W. Zhang, L. Lu, W. Zhang, Y. Wang, S. D. Ware, J. Mondragon, J. Rein, N. Strotman, D. Lehnherr, K. A. See, S. Lin, *Nature* **2022**, *604*, 292–297.
[37] S. Z. Sun, M. Börjesson, R. Martin-Montero, R. Martin, *J. Am. Chem. Soc.* **2018**, *140*, 12765–12769.
[38] D. Wang, C. Mück-Lichtenfeld, A. Studer, *J. Am. Chem. Soc.* **2019**, *141*, 14126–14130.
[39] M. Chierchia, P. Xu, G. J. Lovinger, J. P. Morken, *Angew. Chem. Int. Ed.* **2019**, *58*, 14245–14249.
[40] C. Yang, S. Bai, Y. Gao, Q. Wu, X. Qi, *Chem* **2023**, *9*, https://doi.org/10.1016/j.chempr.2023.04.006.
[41] M. Ueda, Y. Kato, N. Taniguchi, T. Morisaki, *Org. Lett.* **2020**, *22*, 6234–6238.
[42] B. Quiclet-Sire, S. Z. Zard, *J. Am. Chem. Soc.* **2015**, *137*, 6762–6765.
[43] H. Suzuki, T. Nishikawa, H. Makino, M. Ouchi, *Chem. Sci.* **2022**, *13*, 12703–12712.
[44] J. C. Walton, A. J. McCarroll, Q. Chen, B. Carboni, R. Nziengui, *J. Am. Chem. Soc.* **2000**, *122*, 5455–5463.
[45] N. Kumar, R. R. Reddy, N. Eghbarieh, A. Masarwa, *Chem. Commun.* **2020**, *56*, 13–25.
[46] D. J. Henry, C. J. Parkinson, P. M. Mayer, L. Radom, *J. Phys. Chem. A* **2001**, *105*, 6750–6756.
[47] D. J. Pasto, *J. Am. Chem. Soc.* **1988**, *110*, 8164–8175.
[48] L. Yang, D. H. Tan, W. X. Fan, X. G. Liu, J. Q. Wu, Z. S. Huang, Q. Li, H. Wang, *Angew. Chem. Int. Ed.* **2021**, *60*, 3454–3458.
[49] M. B. Coolidge, W. T. Borden, *J. Am. Chem. Soc.* **1988**, *110*, 2298–2299.
[50] M. L. Poutsma, *J. Org. Chem.* **2011**, *76*, 270–276.
[51] M. D. Wodrich, W. C. McKee, P. V. R. Schleyer, *J. Org. Chem.* **2011**, *76*, 2439–2447.
[52] P. C. St. John, Y. Guan, Y. Kim, B. D. Etz, S. Kim, R. S. Paton, *Sci. Data* **2020**, *7*, 244.
[53] Y. Zhao, D. G. Truhlar, *Theor. Chem. Acc.* **2008**, *120*, 215–241.
[54] P. C. St. John, Y. Guan, Y. Kim, S. Kim, R. S. Paton, *Nat. Commun.* **2020**, *11*, 2328.
[55] Trifluoroborate calculations were performed without a counter ion and this could affect RSE.
[56] T. Mancilla, M. de los Ángeles Calixto Romo, L. A. Delgado, *Polyhedron* **2007**, *26*, 1023–1028.
[57] T. Mancilla, R. Contreras, B. Wrackmeyer, *J. Organomet. Chem.* **1986**, *307*, 191–198.
[58] D. J. Blair, S. Chitti, M. Trobe, D. M. Kostyra, H. M. S. Haley, R. L. Hansen, S. G. Ballmer, T. J. Woods, W. Wang, V. Mubayi, M. J. Schmidt, R. W. Pipal, G. F. Morehouse, A. M. E. Palazzolo Ray, D. L. Gray, A. L. Gill, M. D. Burke, *Nature* **2022**, *604*, 92–97.
[59] M. S. Chen, M. C. White, *Science* **2010**, *327*, 566–571.
[60] M. S. Chen, M. C. White, *Science* **2007**, *318*, 783–787.
[61] M. C. White, J. Zhao, *J. Am. Chem. Soc.* **2018**, *140*, 13988–14009.
[62] V. A. Schmidt, R. K. Quinn, A. T. Brusoe, E. J. Alexanian, *J. Am. Chem. Soc.* **2014**, *136*, 14389–14392.
[63] T. Newhouse, P. S. Baran, *Angew. Chem. Int. Ed.* **2011**, *50*, 3362–3374.
[64] M. Zhao, W. Lu, *Org. Lett.* **2018**, *20*, 5264–5267.
[65] Y. Manabe, Y. Kitawaki, M. Nagasaki, K. Fukase, H. Matsubara, Y. Hino, T. Fukuyama, I. Ryu, *Chem. Eur. J.* **2014**, *20*, 12750–12753.
[66] R. K. Quinn, Z. A. Könst, S. E. Michalak, Y. Schmidt, A. R. Szklarski, A. R. Flores, S. Nam, D. A. Horne, C. D. Vanderwal, E. J. Alexanian, *J. Am. Chem. Soc.* **2016**, *138*, 696–702.
[67] Deposition numbers 2284737, 2284738, 2284739, 2284740 contain the supplementary crystallographic data for this paper. These data are provided free of charge by the joint Cambridge Crystallographic Data Centre and Fachinformationszentrum Karlsruhe Access Structures service.
[68] G. S. Hammond, *J. Am. Chem. Soc.* **1955**, *77*, 334–338.
[69] G. A. Russell, H. C. Brown, *J. Am. Chem. Soc.* **1955**, *77*, 4578–4582.
[70] B. A. Glen Russell, H. C. Brown, *J. Am. Chem. Soc.* **1955**, *77*, 4025–4030.
[71] M. S. Kharasch, W. Hered, F. R. Mayo, *J. Org. Chem.* **1941**, *6*, 818–829.
[72] Y. Ji, D. A. DiRocco, J. Kind, C. M. Thiele, R. M. Gschwind, M. Reibarkh, *ChemPhotoChem* **2019**, *3*, 984–992.
[73] C. Feldmeier, H. Bartling, E. Riedle, R. M. Gschwind, *J. Magn. Reson.* **2013**, *232*, 39–44.
[74] W. B. Swords, S. J. Chapman, H. Hofstetter, A. L. Dunn, T. P. Yoon, *J. Org. Chem.* **2022**, *87*, 11776–11782.
[75] K. L. Skubi, W. B. Swords, H. Hofstetter, T. P. Yoon, *ChemPhotoChem* **2020**, *4*, 685–690.
[76] P. Nitschke, N. Lokesh, R. M. Gschwind, *Prog. Nucl. Magn. Reson. Spectrosc.* **2019**, *114–115*, 86–134.

[77] H. E. Bonfield, J. D. Williams, W. X. Ooi, S. G. Leach, W. J. Kerr, L. J. Edwards, *ChemPhotoChem* **2018**, *2*, 938–944.
[78] H. J. Dauben Jr, L. L. McCoy, *J. Am. Chem. Soc.* **1959**, *81*, 4863–4873.
[79] P. Goldfinger, P. A. Gosselain, R. H. Martin, *Nature* **1951**, *168*, 30–32.
[80] K. Quasdorf, J. I. Murray, H. Nguyen, M. V. Silva Elipe, A. Ericson, E. Kircher, L. Guan, S. Caille, *Org. Process Res. Dev.* **2022**, *26*, 458–466.
[81] A. B. Pangborn, M. A. Giardello, R. H. Grubbs, R. K. Rosen, F. J. Rosen, *Organometallics* **1996**, *15*, 1518–1520.
[82] Gaussian 16, Revision C.01, M. J. Frisch, G. W. Trucks, H. B. Schlegel, G. E. Scuseria, M. A. Robb, J. R. Cheeseman, G. Scalmani, V. Barone, G. A. Petersson, H. Nakatsuji, X. Li, M. Caricato, A. V. Marenich, J. Bloino, B. G. Janesko, R. Gomperts, B. Mennucci, H. P. Hratchian, J. V. Ortiz, A. F. Izmaylov, J. L. Sonnenberg, D. Williams-Young, F. Ding, F. Lipparini, F. Egidi, J. Goings, B. Peng, A. Petrone, T. Henderson, D. Ranasinghe, V. G. Zakrzewski, J. Gao, N. Rega, G. Zheng, W. Liang, M. Hada, M. Ehara, K. Toyota, R. Fukuda, J. Hasegawa, M. Ishida, T. Nakajima, Y. Honda, O. Kitao, H. Nakai, T. Vreven, K. Throssell, J. A. Montgomery, Jr., J. E. Peralta, F. Ogliaro, M. J. Bearpark, J. J. Heyd, E. N. Brothers, K. N. Kudin, V. N. Staroverov, T. A. Keith, R. Kobayashi, J. Normand, K. Raghavachari, A. P. Rendell, J. C. Burant, S. S. Iyengar, J. Tomasi, M. Cossi, J. M. Millam, M. Klene, C. Adamo, R. Cammi, J. W. Ochterski, R. L. Martin, K. Morokuma, O. Farkas, J. B. Foresman, D. J. Fox, Gaussian, Inc., Wallingford CT, **2016**.
[83] GaussView, Version 6.1, R. Dennington, T. A. Keith, J. M. Millam, Semichem Inc., Shawnee Mission, KS, **2016**.
[84] S. Grimme, S. Ehrlich, L. Goerigk, *J. Comput. Chem.* **2011**, *32*, 1456–1465.
[85] G. Luchini, J. V. Alegre-Requena, I. Funes-Ardoiz, R. S. Paton, *F1000Research* **2020**, *9*, 291.

Manuscript received: July 5, 2023
Accepted manuscript online: August 4, 2023
Version of record online: August 18, 2023